Role of DTI-MRI parameters in diagnosis of ALS: useful biomarkers for daily practice? Tertiary centre experience and literature review

Edyta Maj[1], Miłosz Jamroży[1], Maksymilian Bielecki[2], Marta Bartoszek[3], Marek Gołębiowski[4], Mikołaj Wojtaszek[5], Magdalena Kuźma-Kozakiewicz[6, 7]

[1]2nd Department of Clinical Radiology, Medical University of Warsaw, Warsaw, Poland
[2]Department of Psychology, SWPS University of Social Sciences and Humanities, Warsaw, Poland
[3]Department of Paediatric Radiology, Paediatric Teaching Clinical Hospital, Medical University of Warsaw, Warsaw, Poland
[4]1st Department of Clinical Radiology, Medical University of Warsaw, Warsaw, Poland
[5]Everlight Radiology, London, United Kingdom
[6]Department of Neurology, Medical University of Warsaw, Warsaw, Poland
[7]Neurodegenerative Diseases Research Group, Medical University of Warsaw, Warsaw, Poland

ABSTRACT

Introduction. Despite the rapid development of neuroimaging techniques, the diagnosis of amyotrophic lateral sclerosis (ALS) remains a significant challenge. Magnetic resonance imaging (MRI) is important for ruling out ALS mimickers, while Diffusion Tensor Imaging (DTI) is a useful tool for the identification of cortical tract damage. The aim of this study was to identify the optimal set of DTI parameters to support the diagnosis of ALS that could be applied to everyday MRI and be used as a disease biomarker in daily practice.

Material and methods. Forty-seven ALS patients and 55 age- and gender-matched healthy individuals underwent MRI using a 1.5-Tesla scanner including a DTI sequence with 30 spatial directions and a b-value 0/1,000 s/mm^2. Two independent researchers measured the DTI parameters: fractional anisotropy (FA), TRACE and apparent diffusion coefficient (ADC) using freehand regions of interest (ROIs) placed along both corticospinal tracts (CSTs), starting at the level of the internal capsule and ending at the medulla.

Results. Statistical significance was only achieved for fractional anisotropy (FA) (ALS vs controls, $p < 0.001$). The highest sensitivity was found in the brainstem (cerebral peduncles, pons and pyramids) where it ranged from 72.3% to 80.9%, whereas the highest specificity was observed at the level of the internal capsule (94.6%). The combined highest sensitivity and specificity was obtained in the pons (72.3% and 72.7%, respectively). Classifier based positive predictive values for Youden index cut-off scores varied between 60.7% and 69.4%.

Conclusions. Fractional anisotropy (FA) measured at the level of the brainstem was shown to be the single most relevant parameter in differentiating patients with ALS from healthy subjects. This has the potential to become an ALS-specific biomarker for patient identification in daily practice.

Key words: amyotrophic lateral sclerosis, neurodegenerative disease, magnetic resonance imaging, diffusion tensor imaging

(*Neurol Neurochir Pol 2022; 56 (6): 490–498*)

Key points

1. Fractional anisotropy (FA) is the best diffusion tensor imaging (DTI) parameter to differentiate between ALS patients and healthy subjects.
2. The highest sensitivity of FA was found in the brainstem (up to 80.9%), while the combined highest sensitivity and specificity was obtained in the pons (72.3% and 72.7%, respectively).
3. Fractional anisotropy (FA) measured at the level of the pons has the potential to become an ALS-specific biomarker for the identification of patients with a clinical suspicion of ALS in daily practice.

Introduction

Amyotrophic lateral sclerosis (ALS) is a fatal neurodegenerative disease affecting the upper (UMN) and lower motor neurons (LMN). Lesions of the UMN are mainly located in the precentral gyrus, corticospinal and corticobulbar tracts, while those of the LMN are predominantly found in the brainstem and anterior horns of the spinal cord. The disease usually involves the extremities in 70% of patients (Limb Onset ALS) or the face (Bulbar Onset ALS) in the remaining 30% of patients [1, 2]. Primary manifestations involve benign hand paresis, foot drop or slurred speech, which within 3-5 years progresses into quadriplegia, anarthria, aphagia and death due to respiratory failure [2, 3]. The diagnosis, according to the revised El Escorial and Awaji criteria, is based on clinical parameters supported by neurophysiological testing, while the role of neuroimaging is restricted to ruling out other diseases with similar clinical symptoms [4].

Hyperintensity in the corticospinal tracts (CSTs), initially seen in the internal capsule on T2-weighted imaging, is usually the first manifestation of ALS in MR [5]. Over time, the entire tract from the motor strip to the spinal cord demonstrates a T2 signal increase and progressive volume loss [6]. Iron deposition in the cortex of the precentral gyrus, known as the 'motor band sign' results in a loss of signal on gradient echo (GRE) and susceptibility-weighted imaging (SWI), but this specific sign is only seen in T2-weighted imaging in approximately 50% of patients [7–9]. In the corticospinal tracts, the specificity of the T2 hyperintensity is above 70% while the sensitivity is below 40% [10] and the 'motor band sign' is observed in 78% of patients in SWI [11]. Importantly, these two features can also be present, to varying degrees, in healthy controls [12].

As the microstructure, biochemistry and metabolism of the central nervous system have been explored in great depth in recent years, advanced neuroimaging techniques such as volume-based morphometry (VBM), magnetic transfer imaging (MTI), quantitative susceptibility mapping (QSM), functional magnetic resonance imaging (fMRI), magnetic resonance spectroscopy (MRS), and single-photon emission computed tomography (SPECT) have become increasingly important in the field of evaluating UMN damage in ALS. At the same time, Diffusion Tensor Imaging (DTI) has become another promising tool in the diagnosis of ALS.

DTI is an advanced MRI technique in which white matter tract integrity can be assessed based on the phenomenon of water molecules diffusion [13]. In physiological conditions, grey matter (GM) and cerebrospinal fluid (CSF) isotropic (identical in all directions) diffusion characteristics change into anisotropic (varied, depending on the direction) diffusion in the white matter (WM) as a result of the different orientation of nerve fibre tracts [14]. To date, DTI has been used to assess WM integrity in physiological conditions, as well as in a variety of WM disorders [15, 16].

In order to observe the progressive damage to the corticospinal and corticobulbar tracts in ALS, a number of studies have attempted to use DTI in quantifying UMN involvement. The first results, published as long ago as 1999 [17], supported the use of diffusion tensor MRI in detecting corticospinal tracts pathology in ALS. Several publications have since demonstrated widespread degeneration of the brain [18–22], while others have focused on the corticospinal tract alone [23–26] using a spectrum of assessment parameters. Several studies have concentrated on fractional anisotropy (FA) [27, 28], while others have explored other DTI parameters such as axial diffusivity (AD), radial diffusivity (RD), and mean diffusivity (MD) [29, 30]. The methodological incongruities in these studies, involving varying MR scanner providers, different field strengths, individual alterations in DTI sequence parameters, and such differing WM diffusion data analysis methods as voxel-based analysis (VBA) and tract-based spatial statistics (TBSS) [31–33], have led to numerous discrepancies in the obtained results.

Although several publications in recent years have showed statistical differences in DTI scalars between ALS affected patients and control subjects, data acquisition using technologically advanced MR units with sophisticated statistical tools and requiring multidisciplinary teams for data analysis is a time consuming process [34], making them tedious and difficult to implement into daily practice.

Clinical rationale for the study

The aim of this study was to assess the differences in DTI parameters along the pyramidal tracts in ALS patients versus healthy controls with the intention of identifying and validating a set of optimal parameters for the diagnosis of ALS which could then be used as disease biomarkers in daily practice.

This study focused on manually measured DTI parameters, obtained using commonly available MR equipment, with standard imaging protocols and acceptable examination times, all of which could be applicable in routine practice.

Material and methods

Patients and controls

One hundred and twenty nine patients (n = 129) with clinically probable and definite ALS according to the El Escorial criteria [3, 4] were diagnosed in our tertiary referral centre between August 2009 and December 2019. After initial review of the available imaging data, 82 patients were rejected from further assessment. The remaining 47 patients with confirmed ALS and adequate imaging quality DTI examinations were included in the study and reviewed further. The control group consisted of 55 age- and gender-matched healthy volunteers with no clinical symptoms. The selected patient group consisted of 30 males and 17 females, mean age 53 years, range 23 to 81. The control group included 29 males and 26 females, mean age 50 years, range 18 to 82. There were no significant differences in gender distribution (p = 0.352) or age (p = 0.357) between patients and controls.

More than 91% of ALS patients presented with Limb Onset ALS, while 8.5% presented with Bulbar Onset ALS. The mean disease duration (defined as the time from the first symptom presentation to the time of MRI examination) was 31 months (range 28 to 136), and mean diagnosis delay (i.e. from onset of first signs of weakness to the formal diagnosis of ALS) was 22 months (range 22 to 26). The median Revised Amyotrophic Lateral Sclerosis Functional Rating Scale (ALSFRS-R) score was 34 (range 24 to 46). At the time of the MR examination, all patients were in a stable general condition and imaging was possible without the use of anaesthesia.

MRI examination

All MRI examinations were acquired using a 1.5-Tesla scanner (Magnetom Avanto SQ Engine TIM 76 × 32, Siemens, Erlangen, Germany), using a 12-channel head coil. The routine protocol consisted of an axial T2 turbo spin echo (TSE) (TR/TE 4,650/85 ms; slice thickness 5 mm), an axial T2 fluid attenuated inversion recovery (FLAIR) (TR/TE/TI 9,000/89/2,500 ms; slice thickness 5 mm), a coronal T2 TSE (TR/TE 4,790/77 ms; slice thickness 5 mm), an axial T1 spin echo (SE) (TR/TE 592/13 ms; slice thickness 5 mm), an axial SWI (TR/TE 49/40 ms; slice thickness 3 mm), a sagittal T2 TSE (TR/TE 3,000/111 ms; slice thickness 5 mm), an axial DWI (TR/TE 4,600/99 ms; slice thickness 5 mm; b-value 0/1,000/2,000 s/mm^2), and a sagittal T1 Magnetisation Prepared Rapid Acquisition Gradient Echo (MPR) (TR/TE 1,720/2.92 ms; slice thickness 1 mm).

DTI was obtained with a spin echo echo-planar pulse sequence with diffusion gradients applied in 30 spatial directions and with the following parameters: TR/TE 3,100/86 ms; slice thickness 5 mm; b-value 0/1,000 s/mm^2; FOV 230 × 230 mm, matrix size 128 × 128 and four averages. The overall scanning time for the DTI acquisition was 6:45 min.

DTI data analysis

Diffusion, in general, is characterised by four main parameters: fractional anisotropy, mean diffusivity, TRACE, and the apparent diffusion coefficient (ADC) [35]. Two of these (FA and ADC) are routinely used. FA indicates anisotropy strength. It ranges from 0 to 1, where 0 denotes isotropic and 1 denotes the highest degree of anisotropic diffusion. In practice, FA values closer to 1 prove a well-organised, dense and integrated structure of the fibres, whereas a decrease in the FA value towards zero indicates a reduction in the tracts' integrity as a result of their damage. The total diffusivity is summarised as TRACE, i.e. the sum of three eigenvalues, which, divided by three, gives mean diffusivity (MD). MD denotes the average diffusion of all directions and is equal to ADC.

All diffusion-tensor imaging data was analysed at a commercially available workstation (Leonardo workstation for MRI, Siemens, Erlangen, Germany). Axial fractional anisotropy (FA) maps were generated. Freehand regions of interest (ROIs) were drawn along both corticospinal tracts: two in the anterior two-thirds of the posterior limb of the internal capsule (IC), one in the middle part of the cerebral peduncles (CP), one in the pons (Pons), and one in the pyramids of the medulla (Pyram). Altogether, 10 ROIs were drawn for each patient and control subject, five on each side. The size of each ROI was adapted to the size of the anatomical structure in a given section; the largest ROI was at the level of the internal capsule where the pyramidal tract has the largest representation, while the smallest ROI was at the level of pyramids, due to the smaller cross-section of medulla oblongata (Fig. 1).
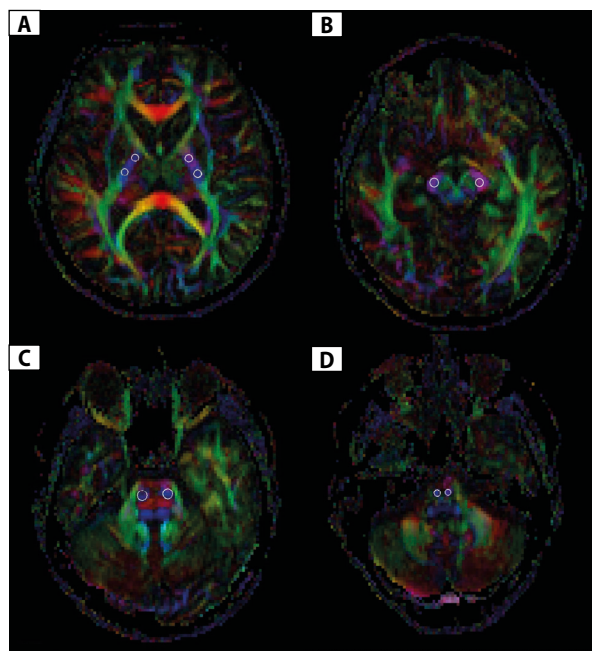

Figure 1. FA maps with ROIs placed on different levels of corticospinal tract: anterior and posterior measurements in anterior two-thirds of posterior limb of both internal capsules (**A**), both sides of cerebral peduncles (**B**), pons (**C**), and pyramids (**D**)

Table 1. Summary results of 2-way mixed design ANOVA. Comparison of mean parameter values taking into account effects of Group, Structure and their interaction. Significant results shown in bold

Parameter	Main effect of Group (ALS vs control)		Main effect of Structure		Group x Structure interaction		Significance of simple effects comparing ALS and controls for each structure				
	F(1, 100)	p	F(4, 400)	p	F(4, 400)	p	IC_p	IC_a	CP	Pons	Pyram
FA	20.23	**< 0.001**	372.84	**< 0.001**	16.94	**< 0.001**	0.615	0.255	**< 0.001**	**< 0.001**	**< 0.001**
ADC	2.24	0.138	112.01	**< 0.001**	5.39	**< 0.001**	0.112	0.659	0.194	**< 0.001**	0.524
TRACE	2.65	0.107	46.92	**< 0.001**	6.26	**< 0.001**	0.113	0.243	**0.006**	0.071	0.067

FA, TRACE and ADC values were obtained for each ROI in order to assess the distribution of DTI parameters along the structures of the pyramidal tracts in patients and control subjects.

Two sets of measurements were performed for each patient and healthy subject by two independent researchers (MJ and MS, radiology trainees) with results expressed as the mean values of the two readings. The standardised voxel size of the ROI for each structure was reproducible and the same for both readers in all patients. There was no time lag between the two independent observer readings. Comparison of mean scores across 'Groups' and 'Structures' was performed using a series of 5 ('Structure': anterior and posterior part of the posterior limb of internal capsule, cerebral peduncle, pons, pyramids) × 2 ('Group': ALS vs control) mixed-design ANOVAs. The 'Group' was a between-subject factor while 'Structure' was a within-subject factor, while the dependent variables consisted of three parameters derived from the obtained DTI measurements: FA, TRACE and ADC (Tab. 1). Results obtained by both observers were averaged prior to analysis. The initial ANOVA also included 'Lateralisation' (left vs. right) as a third independent variable. This factor, however, as it did not affect the other variables, was removed from further analysis. Accordingly, the final ANOVAs were performed on estimates averaged across both sides.

Inter-rater agreement was estimated using the Pearson correlation coefficient. Additionally, for parameters selected following ROC curve analyses, the final cutoff scores were validated. The cutoffs were applied separately to the measurements obtained from each rater, and the quality of the classification based on individual scores was assessed.

Statistical analysis

The R statistical package ver. 3.5.3 (R Core Team, 2019) was used in all analyses.

This study was approved by Medical University of Warsaw institutional review board (number KB 52/2012) and written informed consent was obtained from all patients and controls prior to inclusion in the study.

Results

DTI data

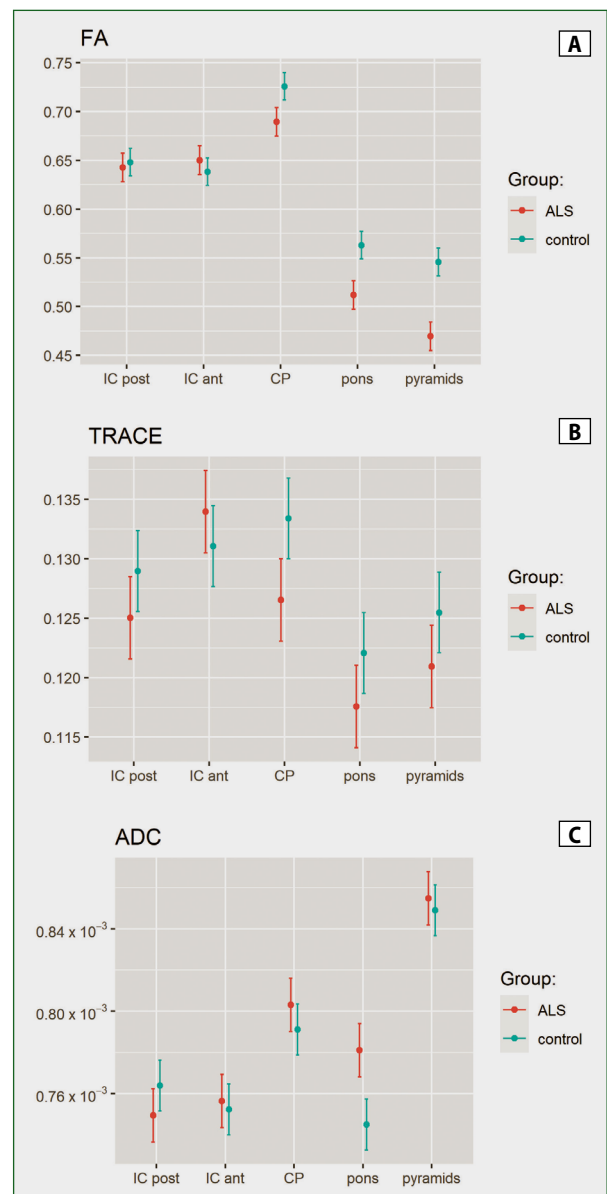Detailed results obtained for all models are set out in Table 1.

Figure 2. Mean FA (**A**), TRACE (**B**), and ADC (**C**) values at different levels of CSTs — comparison of ALS and control groups. Error bars depict 95% confidence intervals.

Only FA parameters for the ALS 'Group' showed statistically significant differences (p < 0.001) with average lower results compared to healthy controls (Fig. 2).

Table 2. ROC curves based on tractography indices for FA and TRACE. Cutoffs were estimated using Youden index. Results with AUC significantly above chance level indicated in bold

Performance of classification based on ROC curve analysis								
FA	**Cut-off**	**Se**	**Sp**	**PPV**	**NPV**	**AUC**	**ll**	**ul**
IC_p	633	55.3%	65.5%	57.8%	63.2%	55.0%	43.7%	66.4%
IC_a	544	6.4%	96.4%	60.0%	54.6%	40.0%	28.8%	51.1%
CP	**714**	**78.7%**	**56.4%**	**60.7%**	**75.6%**	**70.1%**	**59.8%**	**80.3%**
Pons	**522**	**72.3%**	**72.7%**	**69.4%**	**75.5%**	**73.8%**	**63.9%**	**83.7%l**
Pyram	**543**	**80.9%**	**60.0%**	**63.3%**	**78.6%**	**75.2%**	**65.9%**	**84.5%**
TRACE	Cut-off	Se	Sp	PPV	NPV	AUC	ll	ul
IC_p	135	87.2%	43.6%	56.9%	80.0%	60.3%	49.2%	71.5%
IC_a	137	68.1%	43.6%	50.8%	61.5%	46.0%	34.6%	57.3%
CP	**134**	**72.3%**	**61.8%**	**61.8%**	**72.3%**	**65.5%**	**54.8%**	**76.1%**
Pons	**115**	**46.8%**	**78.2%**	**64.7%**	**63.2%**	**61.6%**	**50.6%**	**72.5%**
Pyram	**130**	**83.0%**	**49.1%**	**58.2%**	**77.1%**	**64.9%**	**54.1%**	**75.6%**

IC_p — posterior measurement in anterior two-thirds of posterior limb of internal capsule; IC_a — anterior measurement in anterior two-thirds of posterior limb of internal capsule; CP — cerebral peduncles; Pons — pons; Pyram — pyramids of medulla

For all DTI parameters, the main effects of 'Structure' showed a high statistical significance (all ps < 0.001). Each of these effects was further qualified by an interaction with the Group variable (again, all ps < 0.001), showing that the difference between control subjects and the ALS group varied markedly across structures. The interaction effects were further interpreted using simple effects of Group, which were assessed for each of the relevant structures. The significance of these comparisons is set out in the last five columns of Table 1. In all cases where simple effects were significant, the ALS group means were always below the values observed in the control subjects. For ADC, significant differences were observed in the pons (p < 0.001) and for TRACE in the CP (p < 0.006). The most pronounced differences were observed in FA values, with highly significant effects detected at the level of the pyramids, pons and the cerebral peduncles (all ps < 0.001).

Pearson's r showed strong and very strong correlations between the two observers for TRACE in the brainstem (CP 0.61, Pons 0.83, Pyram 0.69), moderate to strong correlations for FA (CP 0.38, Pons 0.56, Pyram 0.44), and moderate to very weak correlations for ADC (CP 0.26, Pons 0.50, Pyram 0.09). At the level of the IC, satisfactory interrater agreement was observed only for TRACE (ICp 0.59, Ica 0.39) while for the remaining two parameters, correlations were weak (all rs below 0.3).

To summarise, the highest agreement for all three parameters between the two researchers was found in the pons, where there were strong and very strong correlations.

Having considered the diversity of the tested samples in terms of age, the robustness of the ALS effects described above was further assessed by estimating a series of regression models. The obtained results showed that the pattern of results and statistically significant differences between the control and ALS groups remained unchanged after controlling for age effects (n.b. results are not presented for the sake of manuscript brevity).

ROC curve analysis

As the between-group effects were most pronounced for FA scores, we estimated their diagnostic properties using receiver operating characteristics (ROC) analysis. The area under the curve (AUC) values for averaged measurements obtained at the level of the pyramids, pons, and cerebral peduncles were 75.2%, 73.8% and 70.1%, respectively. The positive predictive values for the classifier based on the cut-off scores selected using the Youden index varied between 60.7% and 69.4%. The negative predictive values ranged from 75.5% to 78.6%. The highest sensitivity in FA analysis was found to be in the brainstem (CP, Pons, Pyram) and these ranged from 78.7% to 80.9%, whereas the highest specificity was observed at the level of the internal capsule (94.6%). The results of other parameters were less pronounced (all parameters are set out in Table 2).

To assess the generalisability of the proposed cutoff scores, they were separately applied to the measurements provided by each rater. The sensitivity and the specificity outcomes between the two raters at the level of the CP were very similar (sensitivity 74% *vs.* 70%, specificity 54% *vs.* 56%), moderately differed in the Pyram (78% *vs.* 68% and 60% *vs.* 41% respectively), and were quite divergent in the Pons (72% *vs.* 53% and 58% *vs.* 70% respectively). Not surprisingly, classification based on average scores was superior to the predictions derived from individual radiologists. Of note however, is that classification ratings based on the first and the more experienced of the observers revealed results much closer to the performance of the classification based on averaged ratings.

Discussion

The diagnosis of ALS is mainly based on clinical and electrophysiological assessment. While this is relatively easy if symptoms of both UMN and LMN damage are present, the

primary manifestations of the disease can be misleading [2, 3]. In cases of subtle clinical changes, the involvement of LMN may be confirmed by electrophysiology studies. On the other hand, the results of magnetic stimulation in the assessment of UMN involvement are often inconclusive due to concomitant peripheral damage. According to the revised El Escorial criteria [4], an isolated LMN syndrome is only qualified as suspected ALS, so that patients with this phenotype do not qualify for ALS-registered treatments, nor can they be recruited into clinical trials.

Therefore, there is a need for a quick, simple, readily available and non-invasive neuroimaging tool to support UMN involvement in the diagnosis of ALS [36].

Our study has demonstrated that FA is the best DTI scalar to discriminate between ALS patients and healthy subjects. We have observed a statistically significant reduction in the FA values along the CSTs in ALS individuals compared to the control group, which is in line with previous research [26, 27, 32].

Moreover, we have shown that the effect of Group was the most evident in the brainstem (Fig. 2A), where neuronal fibres are most concentrated, so that the DTI values are more susceptible to structural changes, inducing the most pronounced anisotropy [28]. The highest sensitivity and specificity was found at the level of pons, accounting for 72.3% and 72.7%, respectively. A significant difference between ALS patients and control groups was found in the pons using ADC, and at the cerebral peduncles using TRACE. Using the same measurement method (the ROI approach), Cosottini et al. showed FA decrease in ALS patients along the corticospinal tracts, but those authors did not compare FA values at other CTs levels in their study (Fig 3) [37].

In a systematic review and individual patient data meta-analysis, Foerster at al. estimated DTI diagnostic accuracy measurements in the diagnosis of ALS using corticospinal tract data. In order to minimise heterogeneity, the authors used only average CST or internal capsule (IC) FA data even if studies interrogated other brain regions. The pooled AUC was 75% (95% CI: 66–83), the pooled sensitivity was 68% (95% CI: 62–75), and the pooled specificity was 73% (95% CI: 66–80) [38], which is in line with the results presented in this study (Tab. 2).

In general, most authors have emphasised the role of FA as the main parameter in the diagnosis of ALS patients, agreeing that a decrease in FA indicates an alteration of WM microarchitecture [30].

However, there are differences in results between studies in terms of the areas where the parameter varies. Some authors have identified these to be corticospinal tracts [20, 22, 29, 30, 32, 39], while others have pointed to the brainstem and cerebellar peduncle [30], cerebellum [40, 41], corona radiata, the frontal white matter [29, 42], corpus callosum [41, 43], or even the thalamus [44, 46].

All fibres involved in the motor processes, the motor cortex and commissural fibres are affected in ALS, which is probably
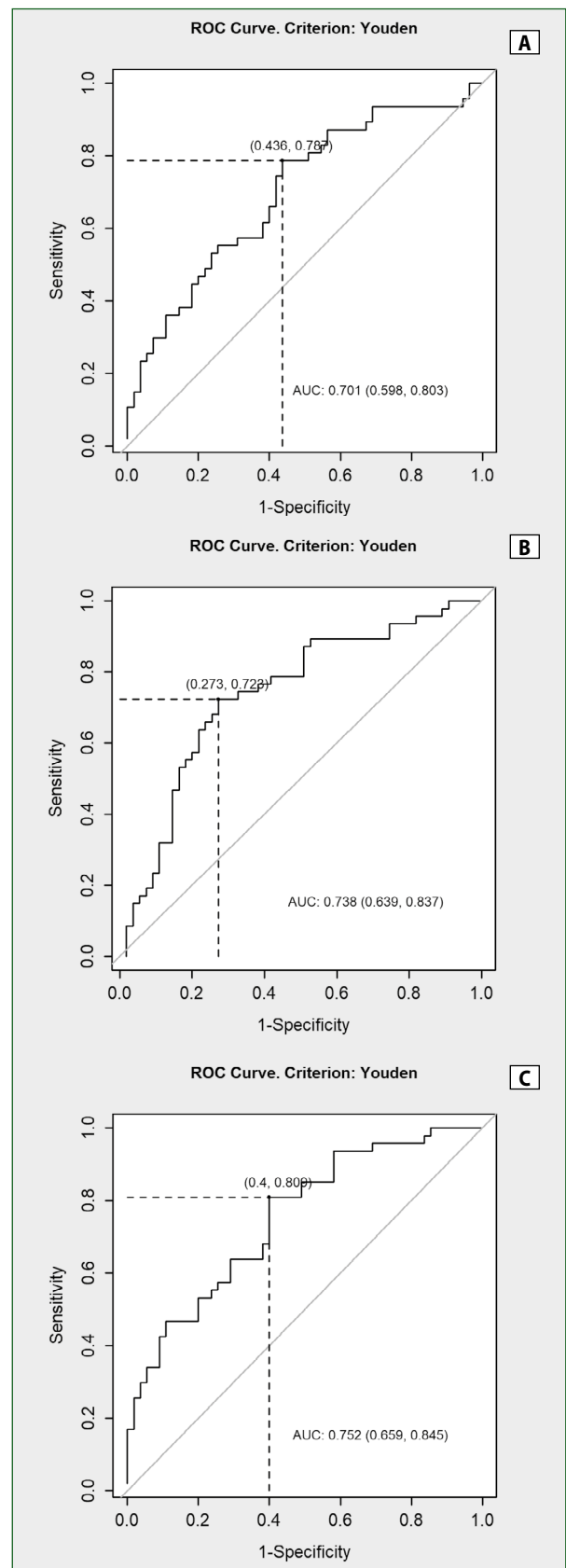

Figure 3. ROC curves illustrate FA values at different levels of brainstem: cerebral peduncles (**A**), pons (**B**), and pyramids (**C**)

due to the white matter microstructure which affects functional connectivity. This was confirmed by Baek at al. when they showed that patients with ALS had widespread changes in DTI values, especially in the CST of the brainstem and cerebellar peduncles, consistent with widespread degeneration of the brain in ALS [30]. A meta-analysis by Zhang et al. proved that neuronal degeneration, rather than being restricted to the corticospinal tracts, also includes the extra-motor areas, which supports the view that ALS is a multisystem degenerative disorder that involves the entire white matter [32]. Our results have further identified the pons as the most sensitive anatomical structure for the diagnosis of ALS.

In recent research, changes in the distribution of DTI-derived metrics have been assessed mainly using TBSS and VBA [20, 29–31, 42, 43]. Sarica et al. suggested univariate tract profile analysis with machine learning to differentiate between ALS patients and healthy subjects [46].

All these publications have confirmed the role of DTI and statistical variations in DTI scalars in ALS patients, but unfortunately, due to high hardware and software requirements, the need for multidisciplinary team data analysis, and the overall time-consuming nature of the process, none of these methods is readily applicable in routine clinical practice.

In the presented study, using easily available tools (ROI approach), we were able to replicate the results of previous research and provide a simple diagnostic method enabling insight into white matter integrity through diffusion tensor scalar assessment, similar to how spectroscopy evaluates metabolites *in vivo*. This could be compared to a non-invasive biopsy – a neuroimaging test we had been looking for to support and accelerate the diagnosis of this rapidly progressing and debilitating disease, especially as we have shown that FA values for patients and healthy controls at the level of brainstem do not overlap.

Our study has several limitations. Firstly, the study group was relatively small, including different patient age subgroup distributions, different disease durations and different disease subtypes, which can all result in varying degrees of pyramidal tracts damage. Any cut-off values presented in this study should be treated with caution, even though no linear correlation between the mean age and disease duration and the FA reductions was shown [29, 32]. There are also substantial discrepancies among authors regarding any correlation between diffusivity measures and ALSFRS-R score: from none [29], through slight [47], to complete correlation [30].

Secondly, even though according to our results, a standard DTI examination and a simple method of DTI parameters analysis could help to distinguish between individuals with ALS and individuals without, there is a caveat that manually drawn ROIs are operator-dependent and not fully reproducible. However, in regions where the pyramidal tract fibres were more densely packed, the correlation between observers was satisfactory which led to a more reliable estimation.

As our results were based on two raters only, a more comprehensive assessment of the cutoffs and generalisability of the proposed algorithm should be warranted in future studies. The comparison of the diagnostic validity of individual ratings showed that more experienced researchers provided higher quality assessments, which suggests that skills and training could further improve the performance of the algorithm.

Finally, it was not possible to compare the defined thresholds to other similar and previously reported in literature values, as, to the best of our knowledge, no data from similar rating and acquisition protocols is available. This is due to differences in patient populations, MRI equipment, and imaging protocols including different TE and b-values as well as different analytical approaches. This highlights the fact that consensus guidelines for ALS MRI studies, such as those proposed by the Neuroimaging Symposium in ALS, are of paramount importance [48]. Moreover, while our study was conducted retrospectively, ideally a larger cohort of patients would be enrolled prospectively to validate these results, using the presented FA range.

Conclusions

Fractional anisotropy (FA) measured at the level of the brainstem was shown to be the single most relevant parameter in differentiating patients with ALS from healthy subjects. In future, this parameter in this location may be a potential ALS-specific biomarker in an ALS diagnostic algorithm for patient identification in daily practice.

Acknowledgements

References

4. Swinnen B, Robberecht W. The phenotypic variability of amyotrophic lateral sclerosis. Nat Rev Neurol. 2014; 10(11): 661–670, doi: 10.1038/nrneurol.2014.184, indexed in Pubmed: 25311585.

5. Kiernan M, Vucic S, Cheah B, et al. Amyotrophic lateral sclerosis. The Lancet. 2011; 377(9769): 942–955, doi: 10.1016/s0140-6736(10)61156-7.

6. Andersen PM, Abrahams S, Borasio GD, et al. EFNS Task Force on Diagnosis and Management of Amyotrophic Lateral Sclerosis:. EFNS guidelines on the clinical management of amyotrophic lateral sclerosis (MALS)--revised report of an EFNS task force. Eur J Neurol. 2012; 19(3): 360–375, doi: 10.1111/j.1468-1331.2011.03501.x, indexed in Pubmed: 21914052.

7. Brooks BR, Miller RG, Swash M, et al. World Federation of Neurology Research Group on Motor Neuron Diseases. El Escorial revisited: revised criteria for the diagnosis of amyotrophic lateral sclerosis. Amyotroph Lateral Scler Other Motor Neuron Disord. 2000; 1(5): 293–299, doi: 10.1080/146608200300079536, indexed in Pubmed: 11464847.

8. Wu RH, Bruening R. Comparison of diffusion-weighted MR imaging and T2-weighted MR imaging in patients with amyotrophic lateral sclerosis. Neuroradiol J. 2007; 19(6): 705–710, doi: 10.1177/197140090601900603, indexed in Pubmed: 24351295.

9. Cheung G, Gawel MJ, Cooper PW, et al. Amyotrophic lateral sclerosis: correlation of clinical and MR imaging findings. Radiology. 1995; 194(1): 263–270, doi: 10.1148/radiology.194.1.7997565, indexed in Pubmed: 7997565.

10. Chakraborty S, Gupta A, Nguyen T, et al. The "motor band sign:" susceptibility-weighted imaging in amyotrophic lateral sclerosis. Can J Neurol Sci. 2015; 42(4): 260–263, doi: 10.1017/cjn.2015.40, indexed in Pubmed: 25971894.

11. Adachi Y, Sato N, Saito Y, et al. Usefulness of SWI for the detection of iron in the motor cortex in amyotrophic lateral sclerosis. J Neuroimaging. 2015; 25(3): 443–451, doi: 10.1111/jon.12127, indexed in Pubmed: 24888543.

12. Kwan JY, Jeong SY, Van Gelderen P, et al. Iron accumulation in deep cortical layers accounts for MRI signal abnormalities in ALS: correlating 7 tesla MRI and pathology. PLoS One. 2012; 7(4): e35241, doi: 10.1371/journal.pone.0035241, indexed in Pubmed: 22529995.

13. Simon NG, Turner MR, Vucic S, et al. Quantifying disease progression in amyotrophic lateral sclerosis. Ann Neurol. 2014; 76(5): 643–657, doi: 10.1002/ana.24273, indexed in Pubmed: 25223628.

14. Roeben B, Wilke C, Bender B, et al. The motor band sign in ALS: presentations and frequencies in a consecutive series of ALS patients. J Neurol Sci. 2019; 406: 116440, doi: 10.1016/j.jns.2019.116440, indexed in Pubmed: 31521959.

15. Ngai S, Tang YM, Du L, et al. Hyperintensity of the precentral gyral subcortical white matter and hypointensity of the precentral gyrus on fluid-attenuated inversion recovery: variation with age and implications for the diagnosis of amyotrophic lateral sclerosis. AJNR Am J Neuroradiol. 2007; 28(2): 250–254, doi: 17296988.

16. Basser PJ, Pierpaoli C, Basser PJ, et al. MR diffusion tensor spectroscopy and imaging. Biophys J. 1994; 66(1): 259–267, doi: 10.1016/S0006-3495(94)80775-1, indexed in Pubmed: 8130344.

17. Mori S, Zhang J. Principles of diffusion tensor imaging and its applications to basic neuroscience research. Neuron. 2006; 51(5): 527–539, doi: 10.1016/j.neuron.2006.08.012, indexed in Pubmed: 16950152.

18. Drake-Pérez M, Boto J, Fitsiori A, et al. Clinical applications of diffusion weighted imaging in neuroradiology. Insights Imaging. 2018; 9(4): 535–547, doi: 10.1007/s13244-018-0624-3, indexed in Pubmed: 29846907.

19. Tae WS, Ham BJ, Pyun SB, et al. Current clinical applications of diffusion-tensor imaging in neurological disorders. J Clin Neurol. 2018; 14(2): 129–140, doi: 10.3988/jcn.2018.14.2.129, indexed in Pubmed: 29504292.

20. Ellis CM, Simmons A, Jones DK, et al. Diffusion tensor MRI assesses corticospinal tract damage in ALS. Neurology. 1999; 53(5): 1051––1058, doi: 10.1212/wnl.53.5.1051, indexed in Pubmed: 10496265.

21. Sarro L, Agosta F, Canu E, et al. Cognitive functions and white matter tract damage in amyotrophic lateral sclerosis: a diffusion tensor tractography study. AJNR Am J Neuroradiol. 2011; 32(10): 1866–1872, doi: 10.3174/ajnr.A2658, indexed in Pubmed: 22016410.

22. Agosta F, Pagani E, Petrolini M, et al. Assessment of white matter tract damage in patients with amyotrophic lateral sclerosis: a diffusion tensor MR imaging tractography study. AJNR Am J Neuroradiol. 2010; 31(8): 1457–1461, doi: 10.3174/ajnr.A2105, indexed in Pubmed: 20395382.

23. Cirillo M, Esposito F, Tedeschi G, et al. Widespread microstructural white matter involvement in amyotrophic lateral sclerosis: a whole--brain DTI study. AJNR Am J Neuroradiol. 2012; 33(6): 1102–1108, doi: 10.3174/ajnr.A2918, indexed in Pubmed: 22300932.

24. Senda J, Kato S, Kaga T, et al. Progressive and widespread brain damage in ALS: MRI voxel-based morphometry and diffusion tensor imaging study. Amyotroph Lateral Scler. 2011; 12(1): 59–69, doi: 10.3109/17482968.2010.517850, indexed in Pubmed: 21271792.

25. Senda J, Ito M, Watanabe H, et al. Correlation between pyramidal tract degeneration and widespread white matter involvement in amyotrophic lateral sclerosis: a study with tractography and diffusion--tensor imaging. Amyotroph Lateral Scler. 2009; 10(5-6): 288–294, doi: 10.3109/17482960802651717, indexed in Pubmed: 19922115.

26. Iwata NK, Aoki S, Okabe S, et al. Evaluation of corticospinal tracts in ALS with diffusion tensor MRI and brainstem stimulation. Neurology. 2008; 70(7): 528–532, doi: 10.1212/01.wnl.0000299186.72374.19, indexed in Pubmed: 18268244.

27. Cosottini M, Giannelli M, Siciliano G, et al. Diffusion-tensor MR imaging of corticospinal tract in amyotrophic lateral sclerosis and progressive muscular atrophy. Radiology. 2005; 237(1): 258–264, doi: 10.1148/radiol.2371041506, indexed in Pubmed: 16183935.

28. Müller HP, Agosta F, Gorges M, et al. Cortico-efferent tract involvement in primary lateral sclerosis and amyotrophic lateral sclerosis: A two-centre tract of interest-based DTI analysis. Neuroimage Clin. 2018; 20: 1062–1069, doi: 10.1016/j.nicl.2018.10.005, indexed in Pubmed: 30343251.

29. Aoki S, Iwata NK, Masutani Y, et al. Quantitative evaluation of the pyramidal tract segmented by diffusion tensor tractography: feasibility study in patients with amyotrophic lateral sclerosis. Radiat Med. 2005; 23(3): 195–199, doi: 15940067.

30. Müller HP, Turner MR, Grosskreutz J, et al. Neuroimaging Society in ALS (NiSALS) DTI Study Group. A large-scale multicentre cerebral diffusion tensor imaging study in amyotrophic lateral sclerosis. J Neurol Neurosurg Psychiatry. 2016; 87(6): 570–579, doi: 10.1136/jnnp-2015-311952, indexed in Pubmed: 26746186.

31. Kassubek J, Müller HP, Del Tredici K, et al. Imaging the pathoanatomy of amyotrophic lateral sclerosis in vivo: targeting a propagation--based biological marker. J Neurol Neurosurg Psychiatry. 2018; 89(4):

374–381, doi: 10.1136/jnnp-2017-316365, indexed in Pubmed: 29101254.

32. Bao Y, Yang L, Chen Y, et al. Radial diffusivity as an imaging biomarker for early diagnosis of non-demented amyotrophic lateral sclerosis. Eur Radiol. 2018; 28(12): 4940–4948, doi: 10.1007/s00330-018-5506-z, indexed in Pubmed: 29948064.

33. Geraldo AF, Pereira J, Nunes P, et al. Beyond fractional anisotropy in amyotrophic lateral sclerosis: the value of mean, axial, and radial diffusivity and its correlation with electrophysiological conductivity changes. Neuroradiology. 2018; 60(5): 505–515, doi: 10.1007/s00234-018-2012-6, indexed in Pubmed: 29564498.

34. Baek SH, Park J, Kim YH, et al. Usefulness of diffusion tensor imaging findings as biomarkers for amyotrophic lateral sclerosis. Sci Rep. 2020; 10(1): 5199, doi: 10.1038/s41598-020-62049-0, indexed in Pubmed: 32251314.

35. Alruwaili AR, Pannek K, Coulthard A, et al. A combined tract-based spatial statistics and voxel-based morphometry study of the first MRI scan after diagnosis of amyotrophic lateral sclerosis with subgroup analysis. J Neuroradiol. 2018; 45(1): 41–48, doi: 10.1016/j.neurad.2017.03.007, indexed in Pubmed: 28802959.

36. Zhang F, Chen G, He M, et al. Altered white matter microarchitecture in amyotrophic lateral sclerosis: A voxel-based meta-analysis of diffusion tensor imaging. Neuroimage Clin. 2018; 19: 122–129, doi: 10.1016/j.nicl.2018.04.005, indexed in Pubmed: 30035009.

37. Kassubek J, Müller HP. Advanced neuroimaging approaches in amyotrophic lateral sclerosis: refining the clinical diagnosis. Expert Rev Neurother. 2020; 20(3): 237–249, doi: 10.1080/14737175.2020.1715798, indexed in Pubmed: 31937156.

38. Basser PJ, Jones DK. Diffusion-tensor MRI: theory, experimental design and data analysis - a technical review. NMR Biomed. 2002; 15(7-8): 456–467, doi: 10.1002/nbm.783, indexed in Pubmed: 12489095.

39. Foerster BR, Welsh RC, Feldman EL. 25 years of neuroimaging in amyotrophic lateral sclerosis. Nat Rev Neurol. 2013; 9(9): 513–524, doi: 10.1038/nrneurol.2013.153, indexed in Pubmed: 23917850.

40. Cosottini M, Giannelli M, Siciliano G, et al. Diffusion-tensor MR imaging of corticospinal tract in amyotrophic lateral sclerosis and progressive muscular atrophy. Radiology. 2005; 237(1): 258–264, doi: 10.1148/radiol.2371041506, indexed in Pubmed: 16183935.

41. Foerster BR, Dwamena BA, Petrou M, et al. Diagnostic accuracy of diffusion tensor imaging in amyotrophic lateral sclerosis: a systematic review and individual patient data meta-analysis. Acad Radiol. 2013; 20(9): 1099–1106, doi: 10.1016/j.acra.2013.03.017, indexed in Pubmed: 23931423.

42. Crespi C, Cerami C, Dodich A, et al. Microstructural white matter correlates of emotion recognition impairment in Amyotrophic Lateral Sclerosis. Cortex. 2014; 53: 1–8, doi: 10.1016/j.cortex.2014.01.002, indexed in Pubmed: 24534360.

43. Tu S, Menke RAL, Talbot K, et al. Cerebellar tract alterations in PLS and ALS. Amyotroph Lateral Scler Frontotemporal Degener. 2019; 20(3-4): 281–284, doi: 10.1080/21678421.2018.1562554, indexed in Pubmed: 30663900.

44. Keil C, Prell T, Peschel T, et al. Longitudinal diffusion tensor imaging in amyotrophic lateral sclerosis. BMC Neurosci. 2012; 13: 141, doi: 10.1186/1471-2202-13-141, indexed in Pubmed: 23134591.

45. Abe O, Yamada H, Masutani Y, et al. Amyotrophic lateral sclerosis: diffusion tensor tractography and voxel-based analysis. NMR Biomed. 2004; 17(6): 411–416, doi: 10.1002/nbm.907, indexed in Pubmed: 15386625.

46. Agosta F, Pagani E, Rocca MA, et al. Voxel-based morphometry study of brain volumetry and diffusivity in amyotrophic lateral sclerosis patients with mild disability. Hum Brain Mapp. 2007; 28(12): 1430–1438, doi: 10.1002/hbm.20364, indexed in Pubmed: 17370339.

47. Thivard L, Pradat PF, Lehéricy S, et al. Diffusion tensor imaging and voxel based morphometry study in amyotrophic lateral sclerosis: relationships with motor disability. J Neurol Neurosurg Psychiatry. 2007; 78(8): 889–892, doi: 10.1136/jnnp.2006.101758, indexed in Pubmed: 17635981.

48. Sach M. Diffusion tensor MRI of early upper motor neuron involvement in amyotrophic lateral sclerosis. Brain. 2004; 127(2): 340–350, doi: 10.1093/brain/awh041.

49. Sarica A, Cerasa A, Valentino P, et al. The corticospinal tract profile in amyotrophic lateral sclerosis. Hum Brain Mapp. 2017; 38(2): 727–739, doi: 10.1002/hbm.23412, indexed in Pubmed: 27659483.

50. Trojsi F, Caiazzo G, Corbo D, et al. Microstructural changes across different clinical milestones of disease in amyotrophic lateral sclerosis. PLoS One. 2015; 10(3): e0119045, doi: 10.1371/journal.pone.0119045, indexed in Pubmed: 25793718.

51. Turner MR, Grosskreutz J, Kassubek J, et al. first Neuroimaging Symosium in ALS (NISALS). Towards a neuroimaging biomarker for amyotrophic lateral sclerosis. Lancet Neurol. 2011; 10(5): 400–403, doi: 10.1016/S1474-4422(11)70049-7, indexed in Pubmed: 21511189.